



## Enhanced vibrational resonance in a single neuron with chemical autapse for signal detection

Zhiwei He(何志威), Chenggui Yao(姚成贵), Jianwei Shuai(帅建伟), and Tadashi Nakano

**Citation:** Chin. Phys. B, 2020, 29 (12): 128702. DOI: 10.1088/1674-1056/abb7

Journal homepage: <http://cpb.iphy.ac.cn>; <http://iopscience.iop.org/cpb>

### What follows is a list of articles you may be interested in

---

## Cross-frequency network analysis of functional brain connectivity in temporal lobe epilepsy

Hai-Tao Yu(于海涛), Li-Hui Cai(蔡立辉), Xin-Yu Wu(武欣昱), Jiang Wang(王江), Jing Liu(刘静), Hong Zhang(张宏)  
Chin. Phys. B, 2019, 28 (4): 048702. DOI: 10.1088/1674-1056/28/4/048702

## Effect of stochastic electromagnetic disturbances on autapse neuronal systems

Liang-Hui Qu(曲良辉), Lin Du(都琳), Zi-Chen Deng(邓子辰), Zi-Lu Cao(曹子露), Hai-Wei Hu(胡海威)  
Chin. Phys. B, 2018, 27 (11): 118707. DOI: 10.1088/1674-1056/27/11/118707

## Firing dynamics of an autaptic neuron

Wang Heng-Tong, Chen Yong

Chin. Phys. B, 2015, 24 (12): 128709. DOI: 10.1088/1674-1056/24/12/128709

## Effects of channel noise on synchronization transitions in delayed scale-free network of stochastic Hodgkin-Huxley neurons

Wang Bao-Ying, Gong Yu-Bing

Chin. Phys. B, 2015, 24 (11): 118702. DOI: 10.1088/1674-1056/24/11/118702

## Adaptive synchronization control of coupled chaotic neurons in the external electrical stimulation

Yu Hai-Tao, Wang Jiang, Deng Bin, Wei Xi-Le, Chen Ying-Yuan

Chin. Phys. B, 2013, 22 (5): 058701. DOI: 10.1088/1674-1056/22/5/058701

---

# CPB

## Chinese Physics B

Volume 29 December 2020 Number 12

**TOPICAL REVIEW**

- Water at molecular level

**SPECIAL TOPIC**

- Twistronics
- Phononics and phonon engineering

A series Journal of the Chinese Physical Society Distributed by IOP Publishing

[iopscience.org/cpb](http://iopscience.org/cpb) | [cpb.iphy.ac.cn](http://cpb.iphy.ac.cn)

**Featured Article**

Peierls-phase-induced topological semimetals in an optical lattice: Moving of Dirac points, anisotropy of Dirac cones, and hidden symmetry protection

Jing-Min Hou

Chin. Phys. B, 2020, 29 (12): 120305

# Chinese Physics B (中国物理 B)

Published monthly in hard copy by the Chinese Physical Society and online by IOP Publishing, Temple Circus, Temple Way, Bristol BS1 6HG, UK

## Institutional subscription information: 2020 volume

For all countries, except the United States, Canada and Central and South America, the subscription rate per annual volume is UK £1326 (electronic only) or UK £1446 (print + electronic).

Delivery is by air-speeded mail from the United Kingdom.

### Orders to:

Journals Subscription Fulfilment, IOP Publishing, Temple Circus, Temple Way, Bristol BS1 6HG, UK

For the United States, Canada and Central and South America, the subscription rate per annual volume is US\$2640 (electronic only) or US\$2870 (print + electronic). Delivery is by transatlantic airfreight and onward mailing.

Orders to: IOP Publishing, P. O. Box 320, Congers, NY 10920-0320, USA

© 2020 Chinese Physical Society and IOP Publishing Ltd

All rights reserved. No part of this publication may be reproduced, stored in a retrieval system, or transmitted in any form or by any means, electronic, mechanical, photocopying, recording or otherwise, without the prior written permission of the copyright owner.

Supported by the China Association for Science and Technology and Chinese Academy of Sciences

**Editorial Office:** Institute of Physics, Chinese Academy of Sciences, P. O. Box 603, Beijing 100190, China  
Tel: (86-10) 82649026 or 82649519, Fax: (86-10) 82649027, E-mail: cpb@aphy.iphy.ac.cn

主管单位: 中国科学院

国际统一刊号: ISSN 1674-1056

主办单位: 中国物理学会和中国科学院物理研究所

国内统一刊号: CN 11-5639/O4

主 编: 欧阳钟灿

编辑部地址: 北京 中关村 中国科学院物理研究所内

出 版: 中国物理学会

通 讯 地 址: 100190 北京 603 信箱

印刷装订: 北京科信印刷有限公司

电 话: (010) 82649026, 82649519

编 辑: Chinese Physics B 编辑部

传 真: (010) 82649027

国内发行: Chinese Physics B 出版发行部

“Chinese Physics B”网址:

国外发行: IOP Publishing Ltd

<http://cpb.iphy.ac.cn>

发行范围: 公开发行

<http://iopscience.iop.org/journal/1674-1056>

## Published by the Chinese Physical Society

### Advisory Board

Prof. Academician Chen Jia-Er(陈佳洱)

School of Physics, Peking University, Beijing 100871, China

Prof. Academician Feng Duan(冯端)

Department of Physics, Nanjing University, Nanjing 210093, China

Prof. Academician T. D. Lee(李政道)

Department of Physics, Columbia University, New York, NY 10027, USA

Prof. Academician Samuel C. C. Ting(丁肇中)

LEP3, CERN, CH-1211, Geneva 23, Switzerland

Prof. Academician C. N. Yang(杨振宁)

Institute for Theoretical Physics, State University of New York, USA

Prof. Academician Yang Fu-Jia(杨福家)

Department of Nuclear Physics, Fudan University, Shanghai 200433, China

Prof. Academician Zhou Guang-Zhao  
(Chou Kuang-Chao)(周光召)

China Association for Science and Technology, Beijing 100863, China

Prof. Academician Wang Nai-Yan(王乃彦)

China Institute of Atomic Energy, Beijing 102413, China

### Editor-in-Chief

Prof. Academician Ouyang Zhong-Can(欧阳钟灿)

Institute of Theoretical Physics, Chinese Academy of Sciences, Beijing 100190, China

## Associate Editors

- Prof. Academician Zhao Zhong-Xian(赵忠贤) Institute of Physics, Chinese Academy of Sciences, Beijing 100190, China  
Prof. Academician Yang Guo-Zhen(杨国桢) Institute of Physics, Chinese Academy of Sciences, Beijing 100190, China  
Prof. Academician Zhang Jie(张杰) Chinese Academy of Sciences, Beijing 100864, China  
Prof. Academician Xing Ding-Yu(邢定钰) Department of Physics, Nanjing University, Nanjing 210093, China  
Prof. Academician Shen Bao-Gen(沈保根) Institute of Physics, Chinese Academy of Sciences, Beijing 100190, China  
Prof. Academician Gong Qi-Huang(龚旗煌) School of Physics, Peking University, Beijing 100871, China  
Prof. Academician Xue Qi-Kun(薛其坤) Department of Physics, Tsinghua University, Beijing 100084, China  
Prof. Sheng Ping(沈平) The Hong Kong University of Science & Technology, Kowloon, Hong Kong, China

## Editorial Board

- Prof. David Andelman School of Physics and Astronomy Tel Aviv University, Tel Aviv 69978, Israel  
Prof. Academician Chen Xian-Hui(陈仙辉) Department of Physics, University of Science and Technology of China, Hefei 230026, China  
Prof. Cheng Jian-Chun(程建春) School of Physics, Nanjing University, Nanjing 210093, China  
Prof. Chia-Ling Chien Department of Physics and Astronomy, The Johns Hopkins University, Baltimore, MD 21218, USA  
Prof. Dai Xi(戴希) Institute of Physics, Chinese Academy of Sciences, Beijing 100190, China  
Prof. Ding Jun(丁军) Department of Materials Science & Engineering, National University of Singapore, Singapore 117576, Singapore  
Prof. Masao Doi Toyota Physical and Chemical Research Institute, Yokomichi, Nagakute, Aichi 480-1192, Japan  
Prof. Fang Zhong(方忠) Institute of Physics, Chinese Academy of Sciences, Beijing 100190, China  
Prof. Feng Shi-Ping(冯世平) Department of Physics, Beijing Normal University, Beijing 100875, China  
Prof. Academician Gao Hong-Jun(高鸿钧) Institute of Physics, Chinese Academy of Sciences, Beijing 100190, China  
Prof. Gu Chang-Zhi(顾长志) Institute of Physics, Chinese Academy of Sciences, Beijing 100190, China  
Prof. Gu Min(顾敏) School of Optical-Electrical and Computer Engineering, University of Shanghai for Science and Technology, Shanghai 200093, China  
Prof. Academician Guo Guang-Can(郭光灿) School of Physical Sciences, University of Science and Technology of China, Hefei 230026, China  
Prof. Academician He Xian-Tu(贺贤土) Institute of Applied Physics and Computational Mathematics, Beijing 100088, China  
Prof. Werner A. Hofer Stephenson Institute for Renewable Energy, The University of Liverpool, Liverpool L69 3BX, UK  
Prof. Hong Ming-Hui(洪明辉) Department of Electrical and Computer Engineering, National University of Singapore, Singapore 117576, Singapore  
Prof. Hu Gang(胡岗) Department of Physics, Beijing Normal University, Beijing 100875, China  
Prof. Jiang Hong-Wen(姜弘文) Department of Physics and Astronomy, University of California, Los Angeles, CA 90095, USA  
Prof. Jiang Ying(江颖) School of Physics, Peking University, Beijing 100871, China  
Prof. Jin Xiao-Feng(金晓峰) Department of Physics, Fudan University, Shanghai 200433, China  
Prof. Robert J. Joynt Physics Department, University of Wisconsin-Madison, Madison, USA  
Prof. Jaewan Kim Korea Institute for Advanced Study, School of Computational Sciences, Hoegiro 85, Seoul 02455, Korea  
Prof. Li Ru-Xin(李儒新) Shanghai Institute of Optics and Fine Mechanics, Chinese Academy of Sciences, Shanghai 201800, China  
Prof. Li Xiao-Guang(李晓光) Department of Physics, University of Science and Technology of China, Hefei 230026, China  
Assits. Prof. Liu Chao-Xing(刘朝星) Department of Physics, Pennsylvania State University, PA 16802-6300, USA  
Prof. Liu Xiang-Yang(刘向阳) Department of Physics, Xiamen University, Xiamen 361005, China  
Prof. Liu Ying(刘荧) Department of Physics and Astronomy, Shanghai Jiao Tong University, Shanghai 200240, China  
Prof. Long Gui-Lu(龙桂鲁) Department of Physics, Tsinghua University, Beijing 100084, China  
Prof. Lv Li(吕力) Institute of Physics, Chinese Academy of Sciences, Beijing 100190, China  
Prof. Ma Xu-Cun(马旭村) Department of Physics, Tsinghua University, Beijing 100084, China  
Prof. Antonio H. Castro Neto Physics Department, Faculty of Science, National University of Singapore, Singapore 117546, Singapore  
Prof. Nie Yu-Xin(聂玉昕) Institute of Physics, Chinese Academy of Sciences, Beijing 100190, China  
Prof. Niu Qian(牛谦) Department of Physics, University of Texas, Austin, TX 78712, USA  
Prof. Academician Ouyang Qi(欧阳颀) School of Physics, Peking University, Beijing 100871, China

- Prof. Academician Pan Jian-Wei(潘建伟) Department of Modern Physics, University of Science and Technology of China, Hefei 230026, China
- Prof. Amalia Patane School of Physics and Astronomy, The University of Nottingham, NG7 2RD, UK
- Prof. Qian Lie-Jia(钱列加) Department of Physics and Astronomy, Shanghai Jiao Tong University, Shanghai 200240, China
- Prof. J. Y. Rhee Department of Physics, Sungkyunkwan University, Suwon, Korea
- Prof. Shen Jian(沈健) Department of Physics, Fudan University, Shanghai 200433, China
- Prof. Shen Yuan-Rang(沈元壤) Lawrence Berkeley National Laboratory, Berkeley, CA 94720, USA
- Prof. Shen Zhi-Xun(沈志勋) Stanford University, Stanford, CA 94305-4045, USA
- Prof. Academician Sun Chang-Pu(孙昌璞) Beijing Computational Science Research Center, China Academy of Engineering Physics, Beijing 100094, China
- Prof. Sun Xiao-Wei(孙小卫) Department of Electrical and Electronic Engineering, Southern University of Science and Technology, Shenzhen 518055, China
- Prof. Sun Xiu-Dong(孙秀冬) Department of Physics, Harbin Institute of Technology, Harbin 150001, China
- Prof. Michiyoshi Tanaka Research Institute for Scientific Measurements, Tohoku University, Katahira 2-1-1, Aoba-ku 980, Sendai, Japan
- Prof. Tong Li-Min(童利民) Department of Optical Engineering, Zhejiang University, Hangzhou 310027, China
- Prof. Tong Peng'er(童彭尔) Department of Physics, The Hong Kong University of Science and Technology, Kowloon, Hong Kong, China
- Prof. Wang Bo-Gen(王伯根) School of Physics, Nanjing University, Nanjing 210093, China
- Prof. Wang Kai-You(王开友) Institute of Semiconductors, Chinese Academy of Sciences, Beijing 100083, China
- Prof. Wang Wei(王炜) School of Physics, Nanjing University, Nanjing 210093, China
- Prof. Wang Ya-Yu(王亚愚) Department of Physics, Tsinghua University, Beijing 100084, China
- Prof. Wang Yu-Peng(王玉鹏) Institute of Physics, Chinese Academy of Sciences, Beijing 100190, China
- Prof. Wang Zhao-Zhong(王肇中) Laboratory for Photonics and Nanostructures (LPN) CNRS-UPR20, Route de Nozay, 91460 Marcoussis, France
- Prof. Academician Wang Wei-Hua(汪卫华) Institute of Physics, Chinese Academy of Sciences, Beijing 100190, China
- Prof. Wei Su-Huai(魏苏淮) Beijing Computational Science Research Center, China Academy of Engineering Physics, Beijing 100094, China
- Prof. Wen Hai-Hu(闻海虎) Department of Physics, Nanjing University, Nanjing 210093, China
- Prof. Wu Nan-Jian(吴南健) Institute of Semiconductors, Chinese Academy of Sciences, Beijing 100083, China
- Prof. Academician Xia Jian-Bai(夏建白) Institute of Semiconductors, Chinese Academy of Sciences, Beijing 100083, China
- Prof. Academician Xiang Tao(向涛) Institute of Physics, Chinese Academy of Sciences, Beijing 100190, China
- Prof. Academician Xie Si-Shen(解思深) Institute of Physics, Chinese Academy of Sciences, Beijing 100190, China
- Prof. Academician Xie Xin-Cheng(谢心澄) Department of Physics, Peking University, Beijing 100871, China
- Prof. Academician Xu Zhi-Zhan(徐至展) Shanghai Institute of Optics and Fine Mechanics, Chinese Academy of Sciences, Shanghai 201800, China
- Assist. Prof. Xu Cen-Ke(许岑珂) Department of Physics, University of California, Santa Barbara, CA 93106, USA
- Prof. Academician Ye Chao-Hui(叶朝辉) Wuhan Institute of Physics and Mathematics, Chinese Academy of Sciences, Wuhan 430071, China
- Prof. Ye Jun(叶军) Department of Physics, University of Colorado, Boulder, Colorado 80309-0440, USA
- Prof. Yu Ming-Yang(郁明阳) Theoretical Physics I, Ruhr University, D-44780 Bochum, Germany
- Prof. Academician Zhan Wen-Long(詹文龙) Chinese Academy of Sciences, Beijing 100864, China
- Prof. Zhang Fu-Chun(张富春) Kavli Institute for Theoretical Sciences, University of Chinese Academy of Sciences, Beijing 100190, China
- Prof. Zhang Xiang(张翔) NSF Nanoscale Science and Engineering Center (NSEC), University of California, Berkeley, CA 94720, USA
- Prof. Zhang Yong(张勇) Electrical and Computer Engineering Department, The University of North Carolina at Charlotte, Charlotte, USA
- Prof. Zhang Zhen-Yu(张振宇) International Center for Quantum Design of Functional Materials, University of Science and Technology of China, Hefei 230026, China
- Prof. Zeng Hao(曾浩) Department of Physics, University at Buffalo, SUNY, Buffalo, NY 14260, USA
- Prof. Zheng Bo(郑波) Physics Department, Zhejiang University, Hangzhou 310027, China
- Prof. Zhou Xing-Jiang(周兴江) Institute of Physics, Chinese Academy of Sciences, Beijing 100190, China
- Prof. Academician Zhu Bang-Fen(朱邦芬) Department of Physics, Tsinghua University, Beijing 100084, China

### Editorial Staff

Wang Jiu-Li(王久丽) (Editorial Director) Cai Jian-Wei(蔡建伟) Zhai Zhen(翟振)

# Enhanced vibrational resonance in a single neuron with chemical autapse for signal detection\*

Zhiwei He(何志威)<sup>1</sup>, Chenggui Yao(姚成贵)<sup>2,†</sup>, Jianwei Shuai(帅建伟)<sup>3,‡</sup>, and Tadashi Nakano<sup>4</sup>

<sup>1</sup>Department of Mathematics, Shaoxing University, Shaoxing 312000, China

<sup>2</sup>College of Mathematics, Physics and Information Engineering, Jiaxing University, Jiaxing 314000, China

<sup>3</sup>Department of Physics, State Key Laboratory of Cellular Stress Biology, Innovation Center for Cell Signaling Network, Xiamen University, Xiamen 361102, China

<sup>4</sup>Graduate School of Frontier Biosciences, Osaka University, 5408570, Japan

(Received 16 July 2020; revised manuscript received 9 August 2020; accepted manuscript online 14 September 2020)

Many animals can detect the multi-frequency signals from their external surroundings. The understanding for underlying mechanism of signal detection can apply the theory of vibrational resonance, in which the moderate high frequency driving can maximize the nonlinear system's response to the low frequency subthreshold signal. In this work, we study the roles of chemical autapse on the vibrational resonance in a single neuron for signal detection. We reveal that the vibrational resonance is strengthened significantly by the inhibitory autapse in the neuron, while it is weakened typically by the excitatory autapse. It is generally believed that the inhibitory synapse has a suppressive effect in neuronal dynamics. However, we find that the detection of the neuron to the low frequency subthreshold signal can be improved greatly by the inhibitory autapse. Our finding indicates that the inhibitory synapse may act constructively on the detection of weak signal in the brain and neuronal system.

**Keywords:** neuronal dynamics, autapse, vibrational resonance, synchronization, time delay

**PACS:** 87.19.lj, 05.45.Xt, 87.19.lm

**DOI:** 10.1088/1674-1056/abb7f9

## 1. Introduction

The multi-frequency signals are prevalent and act an important role in biology.<sup>[1–3]</sup> For hunting and communication, many animals can receive and send out signals with different amplitudes and frequencies. For instance, the high frequency signal with a low frequency envelope is more common in the weakly electric fish who communicates with electric signal with a high frequency about 500–1000 Hz, while the low frequency signals (< 20 Hz) are resulted from external environment and small prey items. These signals can be sensed by the electroreceptors located on the skin surface, which is importance for the fish's electro-communication, navigation, and electrolocation.<sup>[4]</sup> Middleton reported a high frequency signal compounded by a low frequency envelope transmission in a electrosensory system,<sup>[5]</sup> and the response of the pyramidal cell to a high-frequency signal with the social envelope has also been investigated in weakly electric fishes.<sup>[6]</sup> To understand how animals succeed in getting the useful information from the hybrid signals, the neuronal system responding to the high frequency signal with a low frequency envelope has been widely investigated.

Indeed, the detection of weak signal is a challenging task,<sup>[7,8]</sup> because weak signal may be concealed easily by noise. However, the finding of stochastic resonance shows

that noise can improve greatly the detection of subthreshold signal in many nonlinear systems.<sup>[9,10]</sup> Similar to the role of noise in stochastic resonance, the high-frequency signal has a similar effect.<sup>[11–13]</sup> The response of a system to the subthreshold signal with a low frequency can be amplified by the optimal amplitude of the high-frequency signal. This phenomenon was first observed in 2000, and is called a vibrational resonance.<sup>[11]</sup> Since multi-frequency signals are ubiquitous in many fields, vibrational resonance has been intensively investigated also.<sup>[14–18]</sup> The vibrational resonance has been discussed in the CA1 neuron model<sup>[19]</sup> and the relationship between vibrational resonance and phase locking in Hodgkin–Huxley model was investigated.<sup>[20]</sup> It is of great significance to understand the detection of a weak signal in a nonlinear system, and so the effects of stochastic resonance and vibrational resonance have been widely investigated and analyzed in the single neuron<sup>[21–23]</sup> and the neuronal networks.<sup>[24–29]</sup>

As a major structural connection in neuronal systems, synapses also play an extraordinary effect in information propagation, which are classified into electrical synapse and chemical synapse. Autapse, as a special synapse, has been found originally in neocortex by Van der Loos and Glaser in 1972.<sup>[30]</sup> The autapse, which connects a neuron to itself by a branch of its own axon, has been evidenced in the cerebellum, striatum, hippocampus, and neocortex.<sup>[31,32]</sup> Since then, many studies

\*Project supported partially by the National Natural Science Foundation of China (Grant Nos. 11675112, 11705116, 11675134, and 11874310) and the National Natural Science Foundation of China for the 111 Project (Grant No. B16029).

†Corresponding author. E-mail: [yaochenggui2006@126.com](mailto:yaochenggui2006@126.com)

‡Corresponding author. E-mail: [jianweishuai@xmu.edu.cn](mailto:jianweishuai@xmu.edu.cn)

© 2020 Chinese Physical Society and IOP Publishing Ltd

<http://iopscience.iop.org/cpb> <http://cpb.iphy.ac.cn>

have revealed that the autapses have a significant impact on brain functions. For example, Bekkers found that the excitatory autapses can maintain persistent electrical activity in the cerebral cortex.<sup>[33]</sup> The artificial GABAergic autaptic conductances can enhance the precision of firing time in pyramidal neurons,<sup>[34]</sup> and elevate the threshold of evoking action potentials to inhibit the repetitive firing.<sup>[35]</sup> As a fact, a plethora of interesting phenomena have been found with the effect of autapse in the neuronal networks.<sup>[36–48]</sup>

In this work, motivated by the biological function of autapse mentioned above, we study the effects of autapse on the response of a single neuron to external multi-frequency signals. Similar work about the effect of autapse on signal transmission in the neuronal network was discussed in our paper.<sup>[49]</sup> We here are interested in the problem how the inhibitory autapse enhances signal detection and information processing in a signal neuron? Thus, we will investigate the effect of chemical autapse on vibrational resonance in a signal neuron level. We show that the vibrational resonance can be enhanced greatly by an inhibitory autapse for signal detection, while weakened vibrational resonance is observed in the neuron with an excitatory autapse. Such an observation contradicts a popular view that the inhibitory synapse plays typically a suppressive role in neuronal dynamics.<sup>[50,51]</sup>

The structure of the paper is as follows. In Section 2, a mathematical model for a neuron with an autapse is introduced, and a quantitative measurement for vibrational resonance is also included. Section 3 presents the main numerical results. Finally, Section 4 give our conclusions and discussion.

## 2. Model

To reveal the effect of autapse on the neuronal dynamics, we will investigate vibrational resonance in the Hodgkin-Huxley neuron model, the equations are written as<sup>[52]</sup>

$$C_m \frac{dV}{dt} = -(g_K n^4 (V - V_K) + g_{Na} m^3 h (V - V_{Na}) + g_l (V - V_l)) + I_{aut} + I_0 + I_{stimu}, \quad (1a)$$

$$\frac{dm}{dt} = \alpha_m (1.0 - m) - \beta_m m, \quad (1b)$$

$$\frac{dn}{dt} = \alpha_n (1.0 - n) - \beta_n n, \quad (1c)$$

$$\frac{dh}{dt} = \alpha_h (1.0 - h) - \beta_h h, \quad (1d)$$

where  $C_m$  is the cell capacitance,  $V$  represents the membrane potential of neuron,  $g_{Na}$ ,  $g_K$ , and  $g_l$  correspond to the maximum conductances of the sodium, potassium, and leak currents, respectively.  $V_K$ ,  $V_{Na}$ , and  $V_l$  stand for the potassium, sodium, and leakage reversal potentials, respectively.  $I_0$  is a stimulus current.  $I_{stimu} = A \cos(\omega t) + B \cos(\Omega t)$  is the multi-frequency periodic signal, the frequency ratio  $N = \Omega/\omega$ . The  $m$  and  $h$  are gating variables which control the activation and

inactivation of the sodium current, the gating variable  $n$  regulates the activation of the potassium current. These dynamics of the gating variables are controlled by the voltage-dependent rates  $\alpha_x(V)$  and  $\beta_x(V)$  ( $x = m, n, h$ ), which read

$$\alpha_m = \frac{0.1(V + 40)}{1 - e^{-(V+40)/10}}, \quad (2a)$$

$$\beta_m = 4e^{(-V-65)/18}, \quad (2b)$$

$$\alpha_n = \frac{0.01(V + 55)}{1 - e^{-(V+55)/10}}, \quad (2c)$$

$$\beta_n = 0.125e^{-(V+65)/80}, \quad (2d)$$

$$\alpha_h = 0.07e^{-(V+65)/20}, \quad (2e)$$

$$\beta_h = \frac{1.0}{1 + e^{-(V+35)/10}}. \quad (2f)$$

The  $I_{aut}$  is an additional delayed stimulus which stands for the self-feedback current. We only study the effect of the excitatory chemical and inhibitory chemical autapse since it was found in experiment. The electrical autapse is not considered in our work. Different models have been proposed to simulate the chemical synapse, such as the fast threshold modulation (FTM) scheme,<sup>[53]</sup> the sigmoidal function model,<sup>[54]</sup> and the exponential function model.<sup>[55,56]</sup> In the paper, we use the chemical autaptic current with monoexponential functions which is fitted by experimental data,<sup>[57]</sup> it is written as

$$I_{aut} = -G(t - \tau)(V - V_{syn}). \quad (3)$$

Here  $G(t - \tau)$  is the autaptic conductance function,  $\tau$  represents the time delay, and  $V_{syn}$  is the autaptic reversal potential. For excitatory synapse,  $V_{syn}$  is larger than the resting potential for generating an inward current. For inhibitory synapse,  $V_{syn}$  is close to potassium's reversal potential.<sup>[55]</sup> As a result, the values of  $V_{syn} = 0.0$  mV and  $V_{syn} = -80.0$  mV for excitatory and inhibitory synapses are typically used in research, respectively.<sup>[56,58]</sup> The equation of autaptic conductance is modeled as

$$G(t) = g_{syn} \alpha(t - t_{fire}), \quad (4)$$

with

$$\alpha(t) = \frac{t}{t_d} e^{-\frac{t}{t_d}}, \quad (5)$$

where  $t_{fire}$  ( $\sim$  ms) is the spiking time of the neuron,  $g_{syn}$  is the maximum conductance of the autaptic channel, and the parameter  $t_d = 2.0$  ms represents the decay time of the function. Table 1 presents the values of the parameters in our model.

To determine the response of the neuron to a low frequency signal, we calculate  $Q$  defined by

$$\begin{aligned} Q &= \sqrt{Q_s^2 + Q_c^2}, \\ Q_s &= \frac{2}{nT} \int_{T_0}^{T_0+nT} V(t) \sin(\omega t) dt, \\ Q_c &= \frac{2}{nT} \int_{T_0}^{T_0+nT} V(t) \cos(\omega t) dt, \end{aligned} \quad (6)$$

where  $T = 2\pi/\omega$ . We have chosen large values for the tran-

sient evolution  $T_0$  and the average time  $T$  with  $n = 500$ . Clearly, the signal transfer is optimized when the output firing is synchronized by the low frequency signal. Thus, there is a very large value of  $Q$  when such a synchronization occurs.<sup>[19,20]</sup> It is noteworthy that the value of  $Q$  is a propor-

tional function of the Fourier transform coefficient  $F(\omega')$  at  $\omega' = \omega$  ( $F(\omega') = \int_0^{+\infty} e^{-i\omega't} V(t) dt$ ). The advantage of calculation of  $Q$  is that it is convenient and fast. As a fact, we have also calculated the Fourier transform spectrum at  $\omega$ , and it does not change the results.

Table 1. Parameter values.

Parameter	Description	Value
$C_m$	cell membrane capacitance	1.0 mF/cm <sup>2</sup>
$g_{Na}$	the maximum conductance for sodium	120.0 mS/cm <sup>2</sup>
$g_K$	the maximum conductance for potassium	36.0 mS/cm <sup>2</sup>
$g_l$	the maximum leakage conductance	0.3 mS/cm <sup>2</sup>
$V_K$	the reversal potential for potassium	-77.0 mV
$V_{Na}$	the reversal potential for sodium	50.0 mV
$V_l$	leakage reversal potential	-54.0 mV
$I_0$	the constant stimulus current	1.0 $\mu$ A/cm <sup>2</sup>
$V_{syn}$	the autaptic reversal potential	0.0 or -80.0 mV
$\tau$	time delay	0-10 ms
$g_{syn}$	the maximum conductance of autaptic channel	0-6 mS/cm <sup>2</sup>
$A$	the amplitude of weak signal	1.0 $\mu$ A/cm <sup>2</sup>
$B$	the amplitude of high-frequency force	0-600 $\mu$ A/cm <sup>2</sup>
$\omega$	the frequency of weak signal	0.5 ms <sup>-1</sup>
$\Omega$	the frequency of high-frequency force	0.6-10 ms <sup>-1</sup>

### 3. Results

First, we investigate the effect of chemical autapse on the response of a single neuron to the low frequency signal. Figures 1(a) and 1(b) illustrate the value of  $Q$  versus  $B$  with excitatory and inhibitory autapse and without autapse. For the rows from top, middle to bottom,  $\Omega = 1.5, 3\sqrt{3}$ , and 10.0, respectively. For the columns from left to right,  $\tau = 2.0$  and 5.0, respectively. In the paper,  $g_{syn} = 0.0$  indicates non-autapse. One can see that  $Q$  increases with increasing amplitude  $B$  and then decreases after reaching to a maximum, indicating clearly the phenomenon of vibrational resonance. Interestingly, we

find that the values of  $Q$  for the neuron with inhibitory autapse become larger than those without autapse, and the resonance windows for the optimal value of  $B$  with  $Q > 25$  get wider, and the optimal response window for vibrational resonance is shifted to the higher values of  $B$ . The inhibitory autapse can enhance the response of the neuron to the low-frequency sub-threshold signal [Fig. 1(a)]. Whereas the value of  $Q$  is very small for the excitatory autapse (solid green circles). From these figures, one can also find that the strengthening effect of inhibitory autapse on vibrational resonance is general, no matter what value of the frequency ratio  $N = \Omega/\omega$  is.

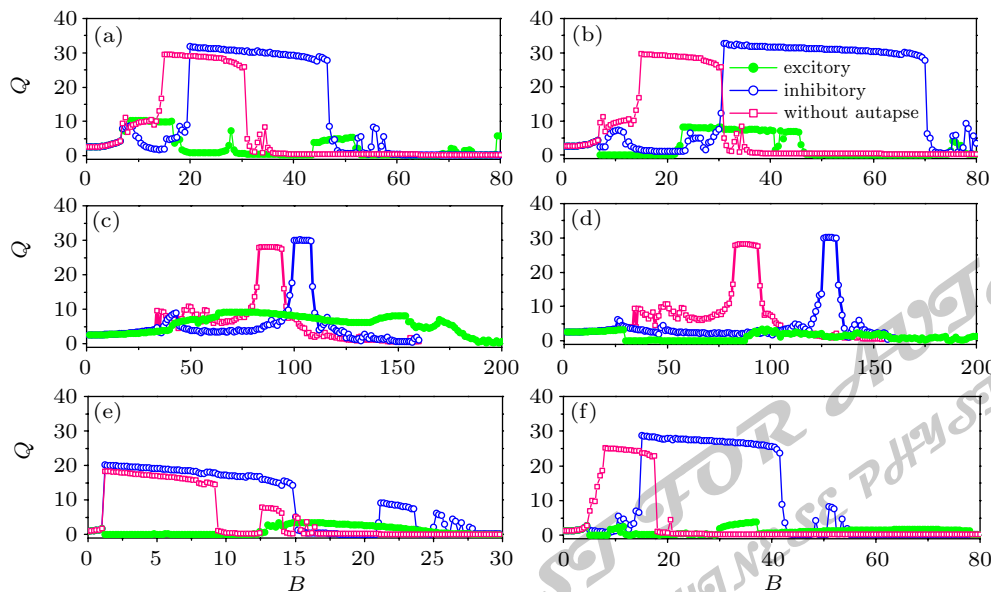


Fig. 1. (a)–(f) The response  $Q$  of neuron against  $B$  without autapse ( $g_{syn} = 0.0$ ) and with excitatory and inhibitory autapses for different parameter settings of  $\tau$  and  $\Omega$ .  $\Omega = 1.5, 3\sqrt{3}$ , and 10.0 corresponds to the top, middle, and bottom rows, respectively. For the left and right columns,  $\tau = 2.0$  and 5.0, respectively. Here,  $g_{syn} = 5.0$ .



To compare globally the deferent effects of excitatory autapse and inhibitory autapse on vibrational resonance, the dependency of  $Q$  on amplitude  $B$  and time delay  $\tau$  is shown for excitatory and inhibitory autapses in Fig. 3, where the color wine represents the occurrence of vibrational resonance with large value of  $Q$  (i.e.,  $Q > 25$ ). From the series of  $V(t)$  of neuron without autapse in Fig. 2, we find  $Q > 25$  ( $Q = 16.76$  when  $B = 14.5$ ,  $Q = 29.49$  when  $B = 16$ .) stands for the situation that the spiking of the neuron is synchronous with the low-frequency signal. In the paper we suggest that  $Q > 25$  stands for the situation that the information of the low-frequency signal can be detected. From Fig. 3, the multiple vibrational resonance which depends sensitively on  $\tau$  and  $B$  is observed clearly for neurons with excitatory or inhibitory autapse. Comparing any three subfigures in each row, however, we find that the size of resonance region which is marked by wine is much bigger for the neuron with the inhibitory autapse than that with the excitatory autapses, showing a stronger response of the neuron with inhibitory autapse to the low frequency signal. Furthermore, we find that the size of the wine region decreases with increasing  $g_{syn}$  for the excitatory autapses, indicating that vibrational resonance is not favored with excitatory autapses.

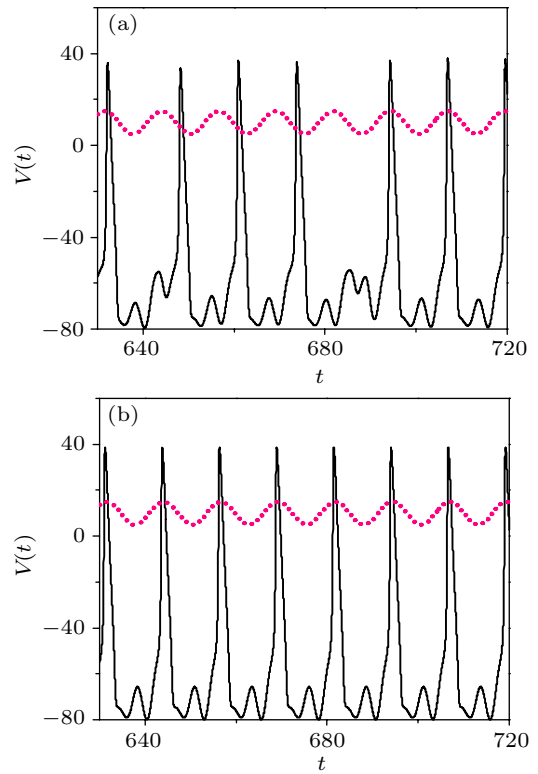


Fig. 2. (a)–(b) Time series of  $V(t)$  of neuron without autapse ( $g_{syn} = 0.0$ ) for  $B = 14.5$  and  $16$ , respectively.  $\omega = 0.5$  and  $\Omega = 1.5$ .

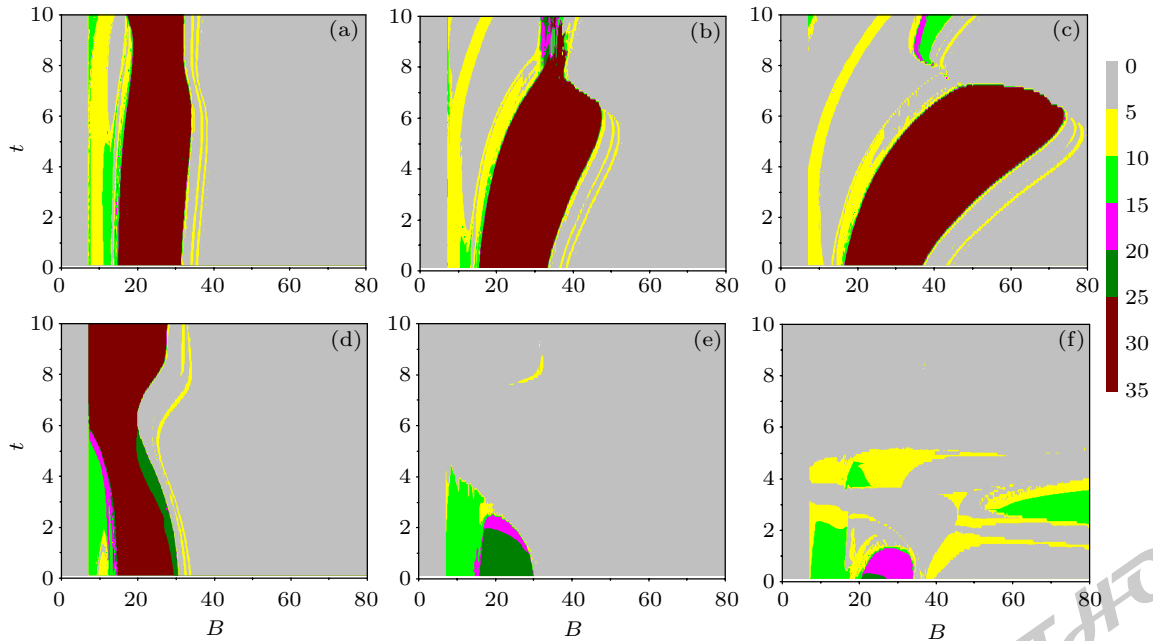


Fig. 3. Contour plots of  $Q$  as a function of  $B$  and  $\tau$  in a neuron with (a)–(c) inhibitory autapse and (d)–(f) excitatory autapse, respectively. From left column to the right column,  $g_{syn} = 0.4, 2.0$ , and  $5.0$ , respectively. Here,  $\omega = 0.5$  and  $\Omega = 1.5$ .

To gain a deeper understanding of the inhibitory-autapse-enhanced vibrational resonance, figure 4 presents the dependence of  $T_i$ , which is defined as the inter-spike interval as a function of  $B$ , for inhibitory (Figs. 4(a)–4(c)) and excitatory autapses (Figs. 4(d)–4(f)). For the columns from left, middle, to right in Fig. 4,  $g_{syn} = 0.4, 2.0$ , and  $5.0$ , respectively. From these figures, one can find that  $T_i$  is multi-valued, indicating aperiodic spiking activities. We have checked carefully the

data of  $T_i$ , but could not find period doubling or expansion with parameter changes. We can observe clearly that some periodical synchronization states occur for excitatory and inhibitory autapses with  $\omega/\omega' = 1:1$  or  $3:2$ , where  $\omega'$  is defined as the frequency of spiking. Interestingly, comparing the three subfigures in each row with increasing  $g_{syn}$ , the periodic synchronization window for  $\omega/\omega' = 1:1$  (i.e., frequency synchronization) gets longer for the neuron with the inhibitory autapse,

while such frequency synchronization is destroyed for the neuron with excitatory autapse. The figures in the middle column show that  $T_i$  decreases tardily to  $T$  ( $T = 2\pi/\omega = 12.56$ ) with increasing  $B$ , which results in the synchronization of the neuron with low-frequency subthreshold signal in the resonance interval.

Further, we show the dynamical phase diagrams on the  $(B, \tau)$  space for excitatory (Figs. 5(a)–5(c)) and inhibitory (Figs. 5(d)–5(f)) autapses with  $g_{\text{syn}} = 0.4, 2.0,$  and  $5.0$  respec-

tively. Based on the observation of spiking, the neuron exhibits three primary features: non-exciting state (NE), aperiodic state (AS), and phase locking state (PL). In Fig. 5, the green region corresponds to AS state, the gray region stands for NE state in which the potential  $V(t)$  fluctuates around a steady state, and the PL states for  $\omega/\omega' = 3:2, 3:4, 1:2,$  and  $1:1$  (frequency synchronization) are marked by dark cyan, pink, yellow, and wine, respectively. The other ratios are marked by orange. Comparing Fig. 5 with Fig. 3, one can find that the regions

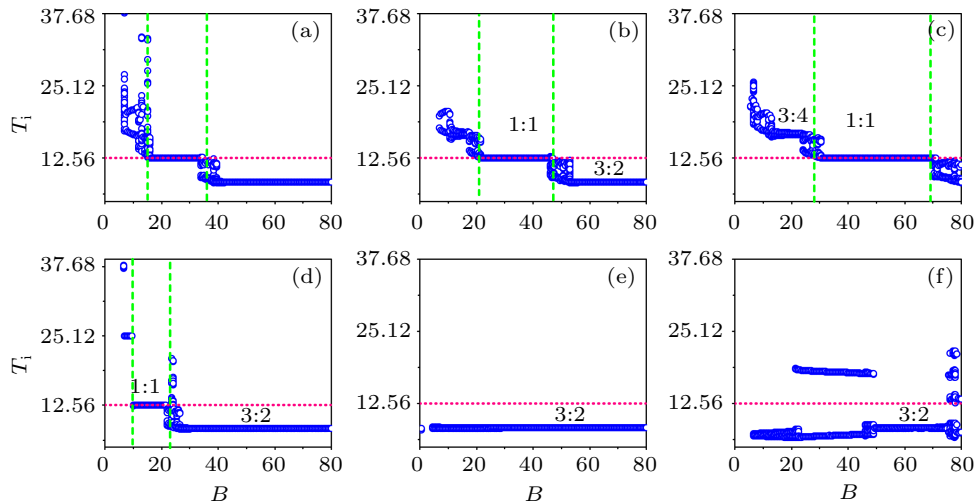


Fig. 4. (a)–(f) The bifurcation diagrams of  $T_i$  which is the interval time of serial spiking. The upper and lower rows correspond to the inhibitory and excitatory autapses, respectively. From the left column to the right column,  $g_{\text{syn}} = 0.4, 2.0,$  and  $5.0$ , respectively. Here  $\tau = 5.0, \omega = 0.5,$  and  $\Omega = 1.5$ .

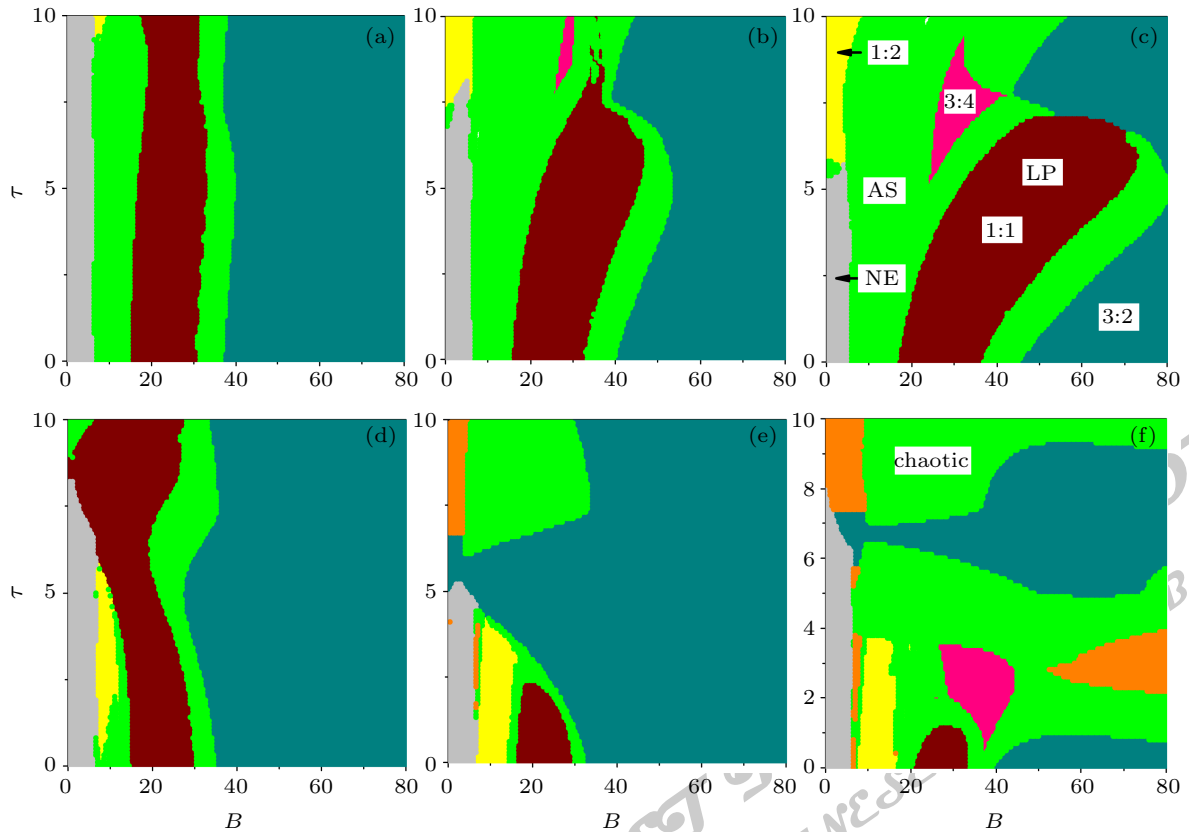


Fig. 5. The dynamical phase diagram on the  $(B, \tau)$  space with (a)–(c) inhibitory and (d)–(f) excitatory autapses for  $g_{\text{syn}} = 0.4, 2.0,$  and  $5.0$  (for left, middle, and right columns), respectively. The letters AS stand for aperiodic state. The letters NE represent non-exciting state where the potential  $V(t)$  fluctuates around the steady state. The 1:1, 1:2, and 3:2 are locking ratios. Here,  $\omega = 0.5$  and  $\Omega = 1.5$ .

with high value of  $Q$  (wine region) are almost the same as those of frequency synchronization, which can be enhanced by the inhibitory autapse, and depend on  $\tau$  and  $B$ . This result suggests that the strengthening effect of inhibitory autapse on vibrational resonance results from the frequency synchronization.

Then, we explore the effect of the maximum conductance of autapse  $g_{syn}$  on the size of the synchronization region in  $(B, \tau)$  space with the rational or irrational ratio of  $\Omega/\omega$ . To quantify the synchronization region, we introduce a normalized scaling factor  $R = S_{FS}/S$ , where  $S_{FS}$  stands for the area of the synchronization region, and  $S$  represents the total area of  $(B, \tau)$  space with  $[0, 80] \times [0, 10]$  (a),  $[0, 200] \times [0, 10]$  (b), and  $[0, 600] \times [0, 10]$  (c), respectively. The results are shown in Fig. 6 for  $\Omega = 1.5, 3\sqrt{3}$ , and  $10.0$ . For excitatory autapse,  $R$  decreases to a small value with the increase of  $g_{syn}$ . Thus, the strong excitatory autapse does not favor the frequency synchronization. Differently,  $R$  holds on a large value for the arbitrary autaptic weight  $g_{syn}$ . The strengthen effect of inhibitory autapse on frequency synchronization is verified again.

Finally, we focus on the regions with a large  $\Omega$ , and discuss the effects of frequency  $\Omega$  on vibrational resonance and frequency synchronization for the neuron. Figures 7(a) and 7(b) give the normalized scaling factor  $R$  as a function of ratio  $N = \Omega/\omega$  for  $g_{syn} = 2.0$  and  $5.0$ , respectively. As shown in Fig. 7, multiple peaks of factor  $R$  are located at integer numbers for excitatory and inhibitory autapses, suggesting that there exists a resonance to the high-frequency force at the driving frequency. One can also find in Fig. 7 that the values of

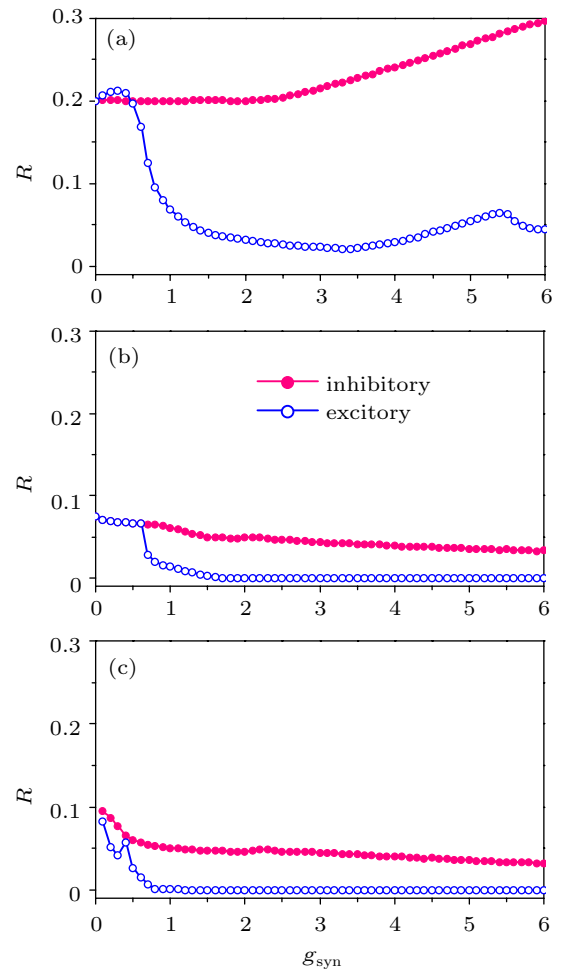


Fig. 6. The normalized scaling factor  $R$  against  $g_{syn}$  for  $\Omega = 1.5$  (a),  $3\sqrt{3}$  (b), and  $10.0$  (c) with excitatory and inhibitory autapses, respectively. Here,  $\omega = 0.5$ .

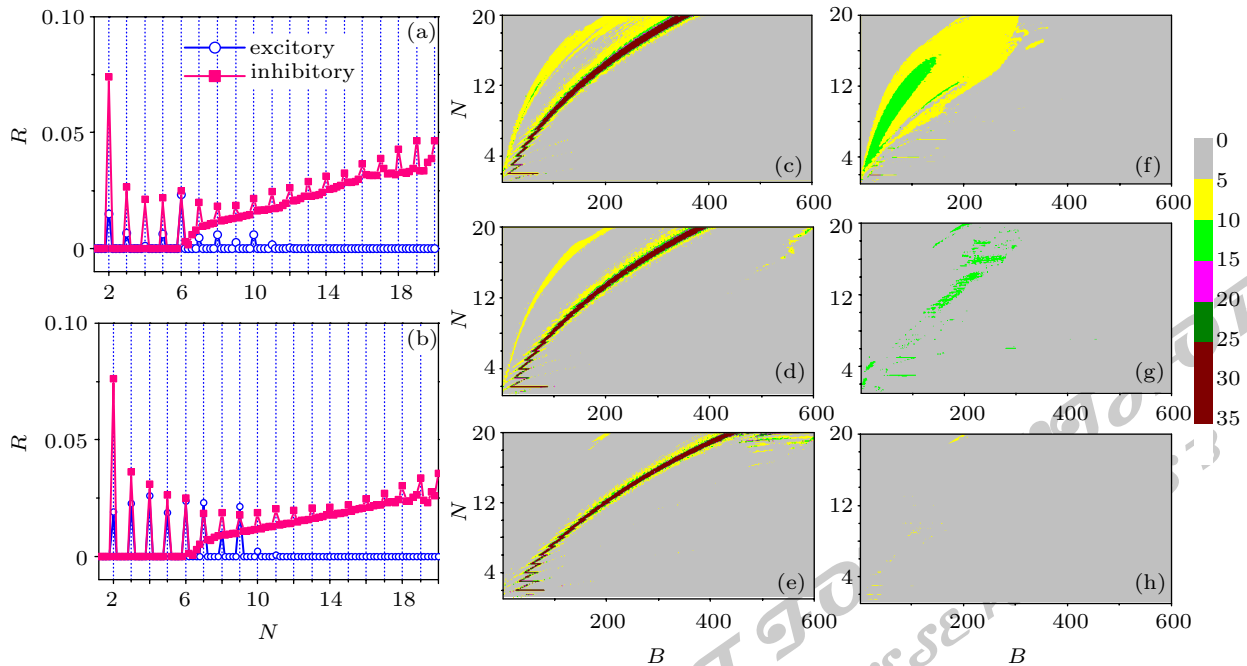


Fig. 7. The normalized factor  $R = S_{FS}/S$  in  $(\tau, B)$  space as a function of  $\Omega$  for  $g_{syn} = 2.0$  (a) and  $5.0$  (b), respectively, where  $S_{FS}$  is the area of region of 1 : 1 phase locking mode, and  $S$  is the area of  $(B, \tau)$  space with  $[0, 600] \times [0, 10]$ . The circles and squares stand for excitatory and inhibitory autapses, respectively. (c)–(h) Contour plots of  $Q$  against  $B$  and  $N$  ( $N = \Omega/\omega$ ) for (c)–(e) inhibitory autapse and (f)–(h) excitatory autapse with different  $N$ , respectively. From top column to bottom column,  $\tau = 1.0, 3.0$ , and  $5.0$ , respectively. Here,  $g_{syn} = 5.0$  and  $\omega = 0.5$ .

peaks for the inhibitory autapse are larger than those for the excitatory autapses at the special frequencies with integer number. Besides these peaks, with the increase of  $N$ , the envelope of  $R$  for the inhibitory autapse increases when  $N$  is over a critical value, while  $R$  for the excitatory autapse vanishes. One also finds inhibitory autapse enhanced vibrational resonance for the large ratio  $N$ . Figures 7(c)–7(h) show the two-dimensional contour plots of  $Q$  as a function of  $B$  and  $N$  with inhibitory autapse (Figs. 7(c)–7(e)) and excitatory autapse (Figs. 7(f)–7(h)), respectively. From these figures, the strengthened vibrational resonance can also be observed for the arbitrary  $\Omega$  with inhibitory autapses, while the weakened effect of excitatory autapse on the vibrational resonance can be verified for the general and incommensurable frequency  $\Omega$ , and the VR with sensitive frequency dependence is justified.

#### 4. Conclusions

We studied in detail the effects of excitatory and inhibitory autapses of a single neuron on the response to the multi-frequency signal. The vibrational resonance can be observed in such a neuron with different autapses, and sensitively depends on system's parameters. Surprisingly, the resonance response of the neuron with an inhibitory autapse becomes stronger than that without autapse. The resonance window gets wider with the inhibitory autapse, while the resonance region is reduced with the excitatory autapse. Thus the vibrational resonance is enhanced by the inhibitory autapse, indicating a strengthened detection of the neuron to the low-frequency signal.

The phase-locking is one of the best known phenomena in the nonlinear system with periodic stimulus. It has been shown that the vibrational resonance can be induced by phase-locking modes in the excitable system.<sup>[20]</sup> The vibrational resonance closely relates with the frequency matching relationship between the neuron with low frequency signal, which is called phase-locking induced vibrational resonance. We find that the inhibitory autapse can achieve 1 : 1 phase-locking mode, which leads to the enhanced vibrational resonance. However, the strong excitatory autapse exterminates the 1 : 1 phase-locking mode. The enhancement of vibrational resonance by the inhibitory autapse is of great interest and may be helpful for us to understand the dynamics of biological systems. Our results present a method to effectively detect the low-frequency signal for neurons with autapse.

The autapse has been found in 80% of cortical pyramidal neurons.<sup>[59]</sup> The biological function of autapse has attracted many researchers' interest and has been extensively investigated. For example, the self-adaption to stimulus can be strengthened by the autapse which is formed due to the contribution of the injury of the neuron.<sup>[60]</sup> The bursting oscillation can be inhibited by the autapse, indicating the improvement of

the adaptive ability of neurons.<sup>[61]</sup> However, what is the role of the autapse in the brain and neural systems is still not completely comprehended. Although the finding of inhibitory-autapse-enhanced vibrational resonance is based on a purely numerical study in the paper, the constructive role of inhibitory autapse on neuronal dynamics, including the vibrational resonances, may be expected to be observed in experiment.

#### Data availability statements

The data used to support the findings of this study are available from the corresponding author on reasonable request.

#### References

- [1] Maksimov A 1997 *Ultrasonics* **35** 79
- [2] Victor J D and Conte M M 2000 *Vis. Neurosci.* **17** 959
- [3] Gherm V, Zernov N, Lundborg B and Vastberg A 1997 *J. Atmos. Sol. Terr. Phys.* **59** 1831
- [4] Heiligenberg W 1991 *Neural Nets in Electric Fish* (Cambridge: MIT Press)
- [5] Middleton J, Longtin A J B and Maler L 2006 *Proc. Natl. Acad. Sci. USA* **103** 14596
- [6] Stamper S A, Fortune E S and Chacron M J 2013 *J. Exp. Biol.* **216** 2393
- [7] Wang G Y and Chen D J 1999 *IEEE Trans. Ind. Electron.* **46** 440
- [8] Modestino J W and Ningo A Y 1979 *Trans. Inform. Theory.* **25** 592
- [9] Wiesenfeld K and Moss F 1995 *Nature* **373** 33
- [10] Gammaitoni L, Hanggi P, Jung P and Marchesoni F 1998 *Rev. Mod. Phys.* **70** 223
- [11] Landa P S and McClintock P V E 2000 *J. Phys. A: Math. Gen.* **33** L433
- [12] Baltanás J P, López L, Blechman I I, Landa P S, Zaikin A, Kurths J and Sanjuán M A F 2003 *Phys. Rev. E* **67** 066119
- [13] Blechman I I and Landa P S 2004 *Int. J. Non-Linear Mech.* **39** 421
- [14] Ullner E, Zaikin A, Garcífa-Ojalvo J, Bascones R and Kurths J 2003 *Phys. Lett. A* **312** 348
- [15] Casado-Pascual J and Baltanás J P 2004 *Phys. Rev. E* **69** 046108
- [16] Yao C G, Liu Y and Zhan M 2011 *Phys. Rev. E* **83** 061122
- [17] Yao C G and Zhan M 2010 *Phys. Rev. E* **81** 061129
- [18] Chizhevsky V N, Smeu E and Giacomelli G 2003 *Phys. Rev. Lett.* **91** 220602
- [19] Wu X X, Yao C G and Shuai J W 2015 *Sci. Rep.* **5** 7684
- [20] Yang L J, Liu W H, Yi M, Wang C J, Zhu Q M, Zhan X and Jia Y 2012 *Phys. Rev. E* **86** 016209
- [21] Kaplan D T, Clay J R, Manning T, Glass L, Guevara M R and Shrier A 1996 *Phys. Rev. Lett.* **76** 4074
- [22] He Z W and Yao C G 2020 *Sci. China Tech. Sc.* **63** 2339
- [23] Yao C G, He Z W, Luo J M and Shuai J W 2015 *Phys. Rev. E* **91** 052901
- [24] Wang L, Zhang P M, Liang P J, Pei J and Qiu Y H 2014 *Chin. Phys. Lett.* **31** 070501
- [25] Ozer M, Uzuntarla M, Kayikcioglu T and Graham L 2008 *J. Phys. Lett. A* **373** 964
- [26] Liang L S, Zhang J Q and Liu L Z 2014 *Chin. Phys. Lett.* **31** 050502
- [27] Yu Y G, Wang W, Wang J F and Liu F 2001 *Phys. Rev. E* **63** 021907
- [28] Zhang X, Huang H B, Li P J, Wu F P, Wu W J and Jiang M 2012 *Chin. Phys. Lett.* **29** 120501
- [29] Cao B, Guan L N and Gu H G 2018 *Acta Phys. Sin.* **67** 240502 (in Chinese)
- [30] Van Der Loos H and Glaser E M 1972 *Brain Res.* **48** 355
- [31] Bekkers J M 1998 *Curr. Biol.* **8** R52
- [32] Flight M H 2009 *Nat. Rev. Neurosci.* **10** 316
- [33] Bekkers J M 2003 *Curr. Biol.* **13** R433
- [34] Bacci A and Huguenard J R 2006 *Neuron* **49** 119
- [35] Bacci A, Huguenard J R and Prince D A 2003 *J. Neurosci.* **23** 859
- [36] Yi M and Yao C G 2020 *Complexity* **2020** 1292417
- [37] Qin H X, Ma J, Wang C N and Wu Y 2014 *PLoS One* **9** e100849
- [38] Wei C L and Zhao X 2019 *Chin. Phys. B* **28** 013201
- [39] Usha K and Subha P A 2019 *Chin. Phys. B* **28** 020502
- [40] Li D X, Bing J and Ye L Y 2019 *Acta Phys. Sin.* **68** 180502 (in Chinese)
- [41] Li Y, Schmid G and Haggi P 2010 *Phys. Rev. E* **82** 061907

- [42] Chen J X, Zhang H, Qiao Li Y, Liang H and Sun W G 2018 *Commun. Nonlinear Sci. Numer. Simulat.* **54** 202
- [43] Yu H T, Cai L H, Wu X Y, Wang J, Liu J and Zhang H 2019 *Chin. Phys. B* **28** 048702
- [44] Yao C G, He Z W, Nakano T and Shuai J W 2018 *Chaos* **28** 083112
- [45] Song X L, Wang H T and Chen Y 2019 *Nonlinear Dyn.* **96** 2341
- [46] Chen J X, Xiao J, Qian L Y and Xu J R 2018 *Nonlinear Sci. Numer. Simul.* **59** 331
- [47] Ma J and Tang J 2019 *Sci. China Tech. Sc.* **62** 2038
- [48] Lv M, Ma J, Yao Y G and Alzahrani F 2015 *Sci. China Tech. Sc.* **58** 448
- [49] Yao C G He Z W and Nakano T 2019 *Nonlinear Dyn.* **97** 1425
- [50] Qian N 1990 *Proc. Natl. Acad. Sci. USA* **87** 8145
- [51] Eccles J C 1982 *Annu. Rev. Neurosci.* **5** 325
- [52] Hodgkin A L and Huxley A F 1952 *J. Physiol.* **117** 500
- [53] Burić N, Todorović K and Vasović N 2008 *Phy. Rev. E* **78** 036211
- [54] Belykh I, Lange E and Hasler M 2005 *Phy. Rev. Lett.* **94** 188101
- [55] Schutter E D 1988 *Computational Modeling Methods for Neuroscientists* (Cambridge: MIT Press)
- [56] Wang S T, Wang W and Liu F 2006 *Phys. Rev. Lett.* **96** 018103
- [57] Connelly W M and Lees G 2010 *J. Physiol.* **588** 2047
- [58] Ozera M, Perc M, Uzuntarla M and Koklukayab E 2010 *NeuroReport* **21** 338
- [59] Lübke J, Markram H, Frotscher M and Sakmann B 1996 *J. Neurosci.* **16** 3209
- [60] Wang C N, Guo S L, Xu Y, Ma J, Tang J Alzahrani F and Aatef H 2017 *Complexity* **2017** 5436737
- [61] Xu Y, Ying H P, Jia Y, Ma J and Hayat T 2017 *Sci. Rep.* **7** 43452

JUST FOR AUTHORS  
— CHINESE PHYSICS B

# Chinese Physics B

Volume 29

Number 12

December 2020

## TOPICAL REVIEW — Water at molecular level

### 126601 Evaporation of nanoscale water on solid surfaces

Rongzheng Wan and Haiping Fang

## TOPICAL REVIEW — Twistronics

### 127304 Progress on band structure engineering of twisted bilayer and two-dimensional moiré heterostructures

Wei Yao, Martin Aeschlimann and Shuyun Zhou

### 128104 A review of experimental advances in twisted graphene moiré superlattice

Yanbang Chu, Le Liu, Yalong Yuan, Cheng Shen, Rong Yang, Dongxia Shi, Wei Yang and Guangyu Zhang

## SPECIAL TOPIC — Twistronics

### 127102 Density wave and topological superconductivity in the magic-angle-twisted bilayer-graphene

Ming Zhang, Yu Zhang, Chen Lu, Wei-Qiang Chen and Fan Yang

## TOPICAL REVIEW — Phononics and phonon engineering

### 126502 Tuning thermal transport via phonon localization in nanostructures

Dengke Ma, Xiuling Li and Lifa Zhang

## SPECIAL TOPIC — Phononics and phonon engineering

### 120505 Nonequilibrium reservoir engineering of a biased coherent conductor for hybrid energy transport in nanojunctions

Bing-Zhong Hu, Lei-Lei Nian and Jing-Tao Lü

### 124402 A phononic rectifier based on carbon schwarzite host-guest system

Zhongwei Zhang, Yulou Ouyang, Jie Chen and Sebastian Volz

### 126303 Reduction of interfacial thermal resistance of overlapped graphene by bonding carbon chains

Yuwen Huang, Wentao Feng, Xiaoxiang Yu, Chengcheng Deng and Nuo Yang

### 126503 Lattice thermal conductivity of $\beta_{12}$ and $\chi_3$ borophene

Jia He, Yulou Ouyang, Cuiqian Yu, Pengfei Jiang, Weijun Ren and Jie Chen

*(Continued on the Bookbinding Inside Back Cover)*

## RAPID COMMUNICATION

- 120301 Double differential cross sections for ionization of H by 75 keV proton impact: Assessing the role of correlated wave functions**  
Jungang Fan, Xiangyang Miao and Xiangfu Jia
- 120305 Peierls-phase-induced topological semimetals in an optical lattice: Moving of Dirac points, anisotropy of Dirac cones, and hidden symmetry protection**  
Jing-Min Hou
- 124207 Realization of ultralow power phase locking by optimizing  $Q$  factor of resonant photodetector**  
Jin-Rong Wang, Hong-Yu Zhang, Zi-Lin Zhao and Yao-Hui Zheng
- 126302 Jamming in confined geometry: Criticality of the jamming transition and implications of structural relaxation in confined supercooled liquids**  
Jun Liu, Hua Tong, Yunhuan Nie and Ning Xu
- 127402 Phase-field simulation of superconductor vortex clustering in the vicinity of ferromagnetic domain bifurcations**  
Hasnain Mehdi Jafri, Jing Wang, Chao Yang, Jun-Sheng Wang and Hou-Bing Huang
- 127404 Structural and electrical transport properties of Cu-doped  $\text{Fe}_{1-x}\text{Cu}_x\text{Se}$  single crystals**  
He Li, Ming-Wei Ma, Shao-Bo Liu, Fang Zhou and Xiao-Li Dong
- 128401 Compact NbN resonators with high kinetic inductance**  
Xing-Yu Wei, Jia-Zheng Pan, Ya-Peng Lu, Jun-Liang Jiang, Zi-Shuo Li, Sheng Lu, Xue-Cou Tu, Qing-Yuan Zhao, Xiao-Qing Jia, Lin Kang, Jian Chen, Chun-Hai Cao, Hua-Bing Wang, Wei-Wei Xu, Guo-Zhu Sun and Pei-Heng Wu
- 128503 Reliability of organic light-emitting diodes in low-temperature environment**  
Saihu Pan, Zhiqiang Zhu, Kangping Liu, Hang Yu, Yingjie Liao, Bin Wei, Redouane Borsali and Kunping Guo
- 128704 Super-resolution filtered ghost imaging with compressed sensing**  
Shao-Ying Meng, Wei-Wei Shi, Jie Ji, Jun-Jie Tao, Qian Fu, Xi-Hao Chen and Ling-An Wu

## GENERAL

- 120201 Rational solutions and interaction solutions for  $(2 + 1)$ -dimensional nonlocal Schrödinger equation**  
Mi Chen and Zhen Wang
- 120302 Chaotic dynamics of complex trajectory and its quantum signature**  
Wen-Lei Zhao, Pengkai Gong, Jiaozhi Wang and Qian Wang
- 120303 Optimal parameter estimation of open quantum systems**  
Yinghua Ji, Qiang Ke and Juju Hu
- 120304 Unconventional photon blockade in a three-mode system with double second-order nonlinear coupling**  
Hong-Yu Lin, Hui Yang and Zhi-Hai Yao

- 120401 A note on the definition of gravitational energy for quadratic curvature gravity via topological regularization**  
Meng-Liang Wang and Jun-Jin Peng
- 120501 Nonlinear resonances phenomena in a modified Josephson junction model**  
Pernel Nguenang, Sandrine Takam Mabekou, Patrick Louodop, Arthur Tsamouo Tsokeng and Martin Tchoffo
- 120502 Localized characteristics of lump and interaction solutions to two extended Jimbo–Miwa equations**  
Yu-Hang Yin, Si-Jia Chen and Xing Lü
- 120503 Energy relaxation in disordered lattice  $\phi^4$  system: The combined effects of disorder and nonlinearity**  
Jianjin Wang, Yong Zhang and Daxing Xiong
- 120504 The landscape and flux of a minimum network motif, Wu Xing**  
Kun Zhang, Ashley Xia and Jin Wang
- 120506 Quantum quenches in the Dicke model: Thermalization and failure of the generalized Gibbs ensemble**  
Xiao-Qiang Su and You-Quan Zhao
- 120701 Fiber cladding SPR bending sensor characterized by two parameters**  
Chunlan Liu, Jiangxi Hu, Yong Wei, Yudong Su, Ping Wu, Lingling Li and Xiaoling Zhao

#### ATOMIC AND MOLECULAR PHYSICS

- 123101 Pressure-dependent physical properties of cubic  $\text{SrBO}_3$  ( $B = \text{Cr, Fe}$ ) perovskites investigated by density functional theory**  
Md Zahid Hasan, Md Rasheduzzaman and Khandaker Monower Hossain
- 123201 Imprint of transient electron localization in  $\text{H}_2^+$  using circularly-polarized laser pulse**  
Jianghua Luo, Jun Li and Huafeng Zhang
- 123701 Interference properties of a trapped atom interferometer in two asymmetric optical dipole traps**  
Li-Yong Wang, Xiao Li, Kun-Peng Wang, Yin-Xue Zhao, Ke Di, Jia-Jia Du and Jian-Gong Hu

#### ELECTROMAGNETISM, OPTICS, ACOUSTICS, HEAT TRANSFER, CLASSICAL MECHANICS, AND FLUID DYNAMICS

- 124201 Two-step phase-shifting Fresnel incoherent correlation holography based on discrete wavelet transform**  
Meng-Ting Wu, Yu Zhang, Ming-Yu Tang, Zhi-Yong Duan, Feng-Ying Ma, Yan-Li Du, Er-Jun Liang and Qiao-Xia Gong
- 124202 Chaotic state as an output of vacuum state evolving in diffusion channel and generation of displaced chaotic state for quantum controlling**  
Feng Chen, Wei Xiong, Bao-Long Fang and Hong-Yi Fan



- 124203 Quantum speed limit time and entanglement in a non-Markovian evolution of spin qubits of coupled quantum dots**  
M. Bagheri Harouni
- 124204 High-dimensional atomic microscopy in surface plasmon polaritons**  
Akhtar Munir, Abdul Wahab and Munsif Jan
- 124205 High-precision three-dimensional atom localization via probe absorption at room temperature**  
Mengmeng Luo, Wenxiao Liu, Dingyu Cai and Shaoyan Gao
- 124206 Generation of atomic spin squeezing via quantum coherence: Heisenberg–Langevin approach**  
Xuping Shao
- 124208 Compound-induced transparency in three-cavity coupled structure**  
Hao-Ye Qin, Yi-Heng Yin and Ming Ding
- 124209 Effect of the distance between focusing lens and target surface on quantitative analysis of Mn element in aluminum alloys by using filament-induced breakdown spectroscopy**  
Xue-Tong Lu, Shang-Yong Zhao, Xun Gao, Kai-Min Guo and Jing-Quan Lin
- 124210 Decoherence of fiber light sources using a single-trench fiber**  
Huahui Zhang, Weili Zhang, Zhao Wang, Hongyang Zhu, Chao Yu, Jiayu Guo, Shanshan Wang and Yunjiang Rao
- 124211 Interference effect on the liquid-crystal-based Stokes polarimeter**  
Jun-Feng Hou, Dong-Guang Wang, Yuan-Yong Deng, Zhi-Yong Zhang and Ying-Zi Sun
- 124212 Absorption, quenching, and enhancement by tracer in acetone/toluene laser-induced fluorescence**  
Guang Chang, Xin Yu, Jiangbo Peng, Yang Yu, Zhen Cao, Long Gao, Minghong Han and Guohua Wu
- 124213 Nonclassicality of photon-modulated atomic coherent states in the Schwinger bosonic realization**  
Jisuo Wang, Xiangguo Meng and Xiaoyan Zhang
- 124301 Impact vibration properties of locally resonant fluid-conveying pipes**  
Bing Hu, Fu-Lei Zhu, Dian-Long Yu, Jiang-Wei Liu, Zhen-Fang Zhang, Jie Zhong and Ji-Hong Wen
- 124401 Calculation of radiative heat flux on irregular boundaries in participating media**  
Yu-Jia Sun and Shu Zheng
- 124501 The (3+1)-dimensional generalized mKdV-ZK equation for ion-acoustic waves in quantum plasmas as well as its non-resonant multiwave solution**  
Xiang-Wen Cheng, Zong-Guo Zhang and Hong-Wei Yang
- 124701 Alternative constitutive relation for momentum transport of extended Navier–Stokes equations**  
Guo-Feng Han, Xiao-Li Liu, Jin Huang, Kumar Nawnit and Liang Sun

**124702 Gravity-capillary waves modulated by linear shear flow in arbitrary water depth**  
Shaofeng Li, Jinbao Song and Anzhou Cao

**124703 Revealing stepping forces in sub-mg tiny insect walking**  
Yelong Zheng, Wei Yin, Hongyu Lu and Yu Tian

**PHYSICS OF GASES, PLASMAS, AND ELECTRIC DISCHARGES**

**125101 Electronic shell study of prolate  $\text{Li}_n$  ( $n = 15\text{--}17$ ) clusters: Magnetic superatomic molecules**  
Lijuan Yan, Jianmei Shao and Yongqiang Li

**125201 Characteristics of DC arcs in a multi-arc generator and their application in the spheroidization of  $\text{SiO}_2$**   
Qifu Lin, Yanjun Zhao, Wenxue Duan, Guohua Ni, Xingyue Jin, Siyuan Sui, Hongbing Xie and Yuedong Meng

**125202 Propagation properties of the chirped Airy–Gaussian vortex electron plasma wave**  
Lican Wu, Jinhong Wu, Yujun Liu and Dongmei Deng

**CONDENSED MATTER: STRUCTURAL, MECHANICAL, AND THERMAL PROPERTIES**

**126101 Anti-oxidation characteristics of Cr-coating on surface of Ti-45Al-8.5Nb alloy by plasma surface metallurgy technique**  
Bing Zhou, Ya-Rong Wang, Ke Zheng, Yong Ma, Yong-Sheng Wang, Sheng-Wang Yu and Yu-Cheng Wu

**126201 Nonperturbative effects of attraction on dynamical behaviors of glass-forming liquids**  
Xiaoyan Sun, Haibo Zhang, Lijin Wang, Zexin Zhang and Yuqiang Ma

**126301 Electronic structure and optical properties of Ge- and F-doped  $\alpha\text{-Ga}_2\text{O}_3$ : First-principles investigations**  
Ti-Kang Shu, Rui-Xia Miao, San-Dong Guo, Shao-Qing Wang, Chen-He Zhao and Xue-Lan Zhang

**126501 Low lattice thermal conductivity and high figure of merit in p-type doped  $\text{K}_3\text{IO}$**   
Weiqiang Wang, Zhenhong Dai, Qi Zhong, Yinchang Zhao and Sheng Meng

**126701 Temperature-dependent Gilbert damping in  $\text{Co}_2\text{FeAl}$  thin films with different B2 ordering degrees**  
Gesang Dunzhu, Yi-Bing Zhao, Ying Jin, Cai Zhou and Chang-Jun Jiang

**CONDENSED MATTER: ELECTRONIC STRUCTURE, ELECTRICAL, MAGNETIC, AND OPTICAL PROPERTIES**

**127101 Characterization and optimization of AlGaN/GaN metal-insulator semiconductor heterostructure field effect transistors using supercritical  $\text{CO}_2/\text{H}_2\text{O}$  technology**  
Meihua Liu, Zhangwei Huang, Kuan-Chang Chang, Xinnan Lin, Lei Li and Yufeng Jin

**127201 Different noncollinear magnetizations on two edges of zigzag graphene nanoribbons**  
Yang Xiao, Qiaoli Ye, Jintao Liang, Xiaohong Yan and Ying Zhang

- 127301 Bound in continuum states and induced transparency in mesoscopic demultiplexer with two outputs**  
Z Labdouti, T Mrabti, A Mouadili, E H El Boudouti, F Fethi and B Djafari-Rouhani
- 127302 Electron dynamics of active mode-locking terahertz quantum cascade laser**  
Qiushi Hou, Chang Wang and Juncheng Cao
- 127303 Tunable metal–insulator transition in  $\text{LaTiO}_3/\text{CaVO}_3$  superlattices: A theoretical study**  
Ya-Kui Weng, Meng-Lan Shen, Jie Li and Xing-Ao Li
- 127401 Multiple reversals of vortex ratchet effects in a superconducting strip with inclined dynamic pinning landscape**  
An He and Cun Xue
- 127403 Thermal stability and thermoelectric properties of Cd-doped nano-layered  $\text{Cu}_2\text{Se}$  prepared using NaCl flux method**  
Jianhua Lu, Decong Li, Wenting Liu, Lanxian Shen, Jiali Chen, Wen Ge and Shukang Deng
- 127501 Improvement of the low-field-induced magnetocaloric effect in  $\text{EuTiO}_3$  compounds**  
Shuang Zeng, Wen-Hao Jiang, Hui Yang, Zhao-Jun Mo, Jun Shen and Lan Li
- 127502 Crystal structure and electromagnetic responses of tetragonal  $\text{GdAlGe}$**   
Cong Wang, Yong-Quan Guo, Tai Wang and Shuo-Wang Yang
- 127701 A novel high breakdown voltage and high switching speed GaN HEMT with p-GaN gate and hybrid AlGaN buffer layer for power electronics applications**  
Yong Liu, Qi Yu and Jiang-Feng Du
- 127801 Improved water oxidation via Fe doping of  $\text{CuWO}_4$  photoanodes: Influence of the Fe source and concentration**  
Yue Sun, Fenqi Du, Donghang Xie, Dongmei Yang, Yang Jiao, Lichao Jia and Haibo Fan
- 127802 Photoluminescence of green InGaN/GaN MQWs grown on pre-wells**  
Shou-Qiang Lai, Qing-Xuan Li, Hao Long, Jin-Zhao Wu, Lei-Ying Ying, Zhi-Wei Zheng, Zhi-Ren Qiu and Bao-Ping Zhang
- INTERDISCIPLINARY PHYSICS AND RELATED AREAS OF SCIENCE AND TECHNOLOGY**
- 128101 Atomistic study on tensile fracture of densified silica glass and its dependence on strain rate**  
Zhi-Qiang Hu, Jian-Li Shao, Yi-Fan Xie and Yong Mei
- 128102 Morphological modifications of  $\text{C}_{60}$  crystal rods under hydrothermal conditions**  
Ming-Run Du, Shi-Xin Liu, Jia-Jun Dong, Ze-Peng Li, Ming-Chao Wang, Tong Wei, Qing-Jun Zhou, Xiong Yang and Peng-fei Shen
- 128103 Effects of  $\text{MgSiO}_3$  on the crystal growth and characteristics of type-Ib gem quality diamond in Fe–Ni–C system**  
Zhi-Yun Lu, Yong-Kui Wang, Shuai Fang, Zheng-Hao Cai, Zhan-Dong Zhao, Chun-Xiao Wang, Hong-An Ma, Liang-Chao Chen and Xiao-Peng Jia

- 128201 Effect of grain boundary energy anisotropy on grain growth in ZK60 alloy using a 3D phase-field modeling**  
Yu-Hao Song, Ming-Tao Wang, Jia Ni, Jian-Feng Jin and Ya-Ping Zong
- 128202 Performance optimization of self-powered visible photodetectors based on Cu<sub>2</sub>O/electrolyte heterojunctions**  
Zhi-Ming Bai, Ying-Hua Zhang, Zhi-An Huang, Yu-Kun Gao and Jia Liu
- 128501 PBTI stress-induced 1/f noise in n-channel FinFET**  
Dan-Yang Chen, Jin-Shun Bi, Kai Xi and Gang Wang
- 128502 A 2DEG back-gated graphene/AlGa<sub>N</sub> deep-ultraviolet photodetector with ultrahigh responsivity**  
Jinhui Gao, Yehao Li, Yuxuan Hu, Zhitong Wang, Anqi Hu and Xia Guo
- 128701 Tail-structure regulated phase behaviors of a lipid bilayer**  
Wenwen Li, Zhao Lin, Bing Yuan and Kai Yang
- 128702 Enhanced vibrational resonance in a single neuron with chemical autapse for signal detection**  
Zhiwei He, Chenggui Yao, Jianwei Shuai and Tadashi Nakano
- 128703 Dielectric properties of nucleated erythrocytes as simulated by the double spherical-shell model**  
Jia Xu, Weizhen Xie, Yiyong Chen, Lihong Wang and Qing Ma
- 128801 A 9% efficiency of flexible Mo-foil-based Cu<sub>2</sub>ZnSn(S, Se)<sub>4</sub> solar cells by improving CdS buffer layer and heterojunction interface**  
Quan-Zhen Sun, Hong-Jie Jia, Shu-Ying Cheng, Hui Deng, Qiong Yan, Bi-Wen Duan, Cai-Xia Zhang, Qiao Zheng, Zhi-Yuan Yang, Yan-Hong Luo, Qing-Bo Men and Shu-Juan Huang
- 128901 Modularity-based representation learning for networks**  
Jialin He, Dongmei Li and Yuexi Liu
- 128902 Shortest path of temporal networks: An information spreading-based approach**  
Yixin Ma, Xiaoyu Xue, Meng Cai and Wei Wang

JUST FOR AUTHORS  
— CHINESE PHYSICS B